Promoter Effect of Early Stage Grown Surface Oxides: A Near- Ambient-Pressure XPS Study of CO Oxidation on PtSn Bimetallics

ARTICLE *in* JOURNAL OF PHYSICAL CHEMISTRY LETTERS · NOVEMBER 2012

Impact Factor: 7.46 · DOI: 10.1021/jz301802g

THE JOURNAL OF PHYSICAL CHEMISTRY Letters

Letter

pubs.acs.org/JPCL

Promoter Effect of Early Stage Grown Surface Oxides: A Near-Ambient-Pressure XPS Study of CO Oxidation on PtSn Bimetallics

Yvette Jugnet,*[,†] David Loffreda,[‡] Céline Dupont,[‡,†] Françoise Delbecq,[‡] Eric Ehret,[†] Francisco J. Cadete Santos Aires,[†] Bongjin S. Mun,[¶] Funda Aksoy Akgul,[§,∥] and Zhi Liu[∥]

[†]Institut de Recherche sur la Catalyse et l'Environnement de Lyon, UMR 5256 CNRS-Université Lyon 1, 69626 Villeurbanne Cedex, France

[‡]Ecole Normale Supérieure de Lyon, Laboratoire de Chimie, UMR 5182 CNRS-Université de Lyon, 69364 Lyon Cedex 07, France

[¶]Department of Applied Physics, Hanyang University, ERICA, Korea 426-791

[§]Department of Physics, Faculty of Arts and Sciences, Nigde University, 51240 Nigde, Turkey

[∥]Advanced Light Source, Lawrence Berkeley National Laboratory, Berkeley, California 94720, United States

Supporting Information

ABSTRACT: The knowledge of the catalyst active phase on the atomic scale under realistic working conditions is the key for designing new and more efficient materials. In this context, the investigation of CO oxidation on the bimetallic $Pt_3Sn(111)$ surfaces by near-ambient-pressure X-ray photoelectron spectroscopy and density functional theory calculations illustrates how combining advanced methodologies allows the determination of the nature of the active phase. Starting from 300 K and 500 mTorr of oxygen, the progressive formation of surface oxides is observed with increasing temperature: SnO, PtO units first, and SnO_2, PtO_2 units afterward. For CO oxidation on the (2×2) surface, the activity gain is assigned to the build-up of ultrathin domains composed of SnO and SnO_2 units. The formation of these early stage surface oxides is entirely supported by a density functional theory analysis. More generally, this study demonstrates how the catalyst surface oxidation and transformation can be better controlled by a relevant choice of environmental conditions.

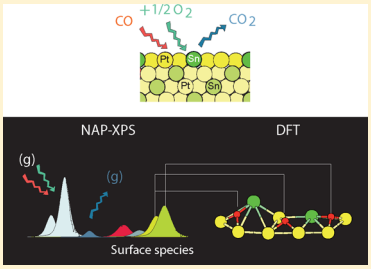

SECTION: Surfaces, Interfaces, Porous Materials, and Catalysis

For many reactions in heterogeneous catalysis, the nature of the active site is often unknown and its determination is greatly challenging. For instance, in most of the catalytic oxidation reactions, the presence and the role of an oxide phase in contact with transition metals is widely debated.[1−4] In this context, the CO oxidation is a probative example for which the chemical nature of the interface is far from being elucidated. In fact it is among the most studied reactions because of its relevance in many industrial applications, such as CO abatement in fuel cells, automotive exhausts, and air cleaning. This entirely justifies the ongoing enthusiasm for investigating this reaction with advanced techniques performed under realistic conditions.[4−9]

The question of the nature of the active phase is usually addressed on monometallic catalysts; however, such a question is even more relevant for bimetallic systems where the presence of the second metal adds a further interesting complexity. Among the most promising materials, PtSn systems have already given rise to exciting experimental and theoretical studies,[10−21] mainly as Pt_3Sn, either bulk or surface alloy. Compared with pure Pt generally used as anode material in fuel cells, this alloy is expected to decrease the CO poisoning effect.

After previous investigations under ultra high vacuum (UHV),[13−19] studies have been performed recently under realistic conditions, thanks to the development of environmental surface instruments. Combining polarization modulation infrared reflection absorption spectroscopy (PM-IRRAS) under elevated pressure of reactants and mass spectroscopy, we have shown a higher efficiency of $Pt_3Sn(111)$ compared with pure Pt(111) in the CO oxidation reaction.[20] In addition, this study revealed a better catalytic performance for the reconstructed (2×2) surface than for the $(\sqrt{3} \times \sqrt{3})$ one. In this study, the influence of oxygen on the CO oxidation was considered only indirectly through the CO-induced perturbations. Indeed, many questions about the oxygen behavior on this alloy remain unanswered: surface composition, segregation phenomena, role of tin, and oxidation state of Sn and Pt. The enhancement of the catalytic performance has been observed without really understanding its origin from the experimental point of view. Several attempts have been tried to advance on the question of the surface oxidation. The oxidation of PtSn surface alloy by oxygen under moderately high pressure at 380−425 K has shown the formation of "quasimetallic" SnO_x $(x < 1)$ and oxidic (SnO or SnO_x with $x < 2$) species.[22] However, the situation should be different in the case of the bulk alloy because it can be considered as a reservoir of tin

Received: November 6, 2012
Accepted: November 29, 2012
Published: November 29, 2012

atoms able to segregate to the surface and to be oxidized. On the basis of theoretical predictions,[23] we expect the adsorption of atomic oxygen on mixed Pt_2Sn sites, with a deep surface restructuring and the buildup of SnO_2 entities induced by oxygen at high coverage. Hence, solving this oxidation process appears as an essential step toward the elucidation of the active site, of the mechanism and of the origin of the enhanced activity for CO oxidation.

Within this context, we study the carbon monoxide oxidation on $Pt_3Sn(111)$ surfaces under elevated pressure conditions by near-ambient-pressure X-ray photoelectron spectroscopy (NAP-XPS). This technique exhibits a unique capacity of following simultaneously all of the reaction partners under working conditions, namely, the substrate (potential segregation of one of the components of the alloy, electronic charge transfer, oxidation state), the surface species (chemical state, bonding to the substrate, etc.), and the gas phase. The interpretation is supported by a density functional theory (DFT) analysis.

The NAP-XPS experiments were performed at the beamline 9.3.2. of the Advanced Light Source at Berkeley in a system previously described.[24] The $Pt_3Sn(111)$-(2×2) and -$(\sqrt{3} \times \sqrt{3})$ surfaces were prepared by conventional UHV procedures.[20] The in situ XPS measurements were performed under flow of reactants. The gas-phase composition was monitored continuously by mass spectroscopy. The DFT calculations were performed under periodic boundary conditions (VASP 4.6[25,26]) with the Perdew–Burke–Ernzerhof[27] exchange correlation GGA functional and the projector-augmented wave method.[28] The Kohn–Sham one-electron equations were solved on the basis of plane waves with kinetic energies below 400 eV. A $(2\sqrt{3} \times 2\sqrt{3})$ supercell was selected to describe the (2×2) termination (five metallic layer slabs). Core level binding energy (CLBE) shifts were calculated in the final state approximation. All technical details of experimental methods and ab initio calculations are reported in the Supporting Information (SI), together with a complete XPS characterization of the clean surfaces, including the surface core level shifts (SCLSs). In this letter, only the results of the most active (2×2) surface are exposed; those relative to the $(\sqrt{3} \times \sqrt{3})$ are addressed in the SI.

In a first step, we report on the effect of oxygen pressure on the alloy surface at various temperatures. The evolution of Sn3d, Pt4f, and O1s core levels with temperature under oxygen pressure is reported in Figures 1 and 2. A 500 mTorr O_2 exposure at 300 K induces an attenuation of the Sn3d and Pt4f surface components (see Figure 1) to the benefit of new features observed at 71.8 and 73.0 eV on $Pt4f_{7/2}$ and at 486.6 eV on $Sn3d_{5/2}$. On the low BE side of the O_2 gas-phase doublet centered at ~537.8 eV, the O1s core level (see Figure 2) rather broad and asymmetric can be resolved into three components at 529.25, 530.15, and 531.4 eV. From the similarity among Pt4f (71.8 eV), Sn3d (486.6 eV), and O1s (529.25 eV) behaviors observed when temperature is progressively increased to 423 K, we assign these components to chemisorbed atomic oxygen O_{ads}. This state induces a positive core level shift of +0.65 and +1 eV on Pt4f and Sn3d, respectively. The evolution with temperature of Pt4f, Sn3d, and O1s core levels is now interpreted on the basis of theoretical predictions.

DFT calculations of atomic oxygen adsorption on this (2×2) termination have been considered with various surface coverages (1/12–1/2 ML).[23] The corresponding CLBEs have been investigated and the complete set of results is exposed in

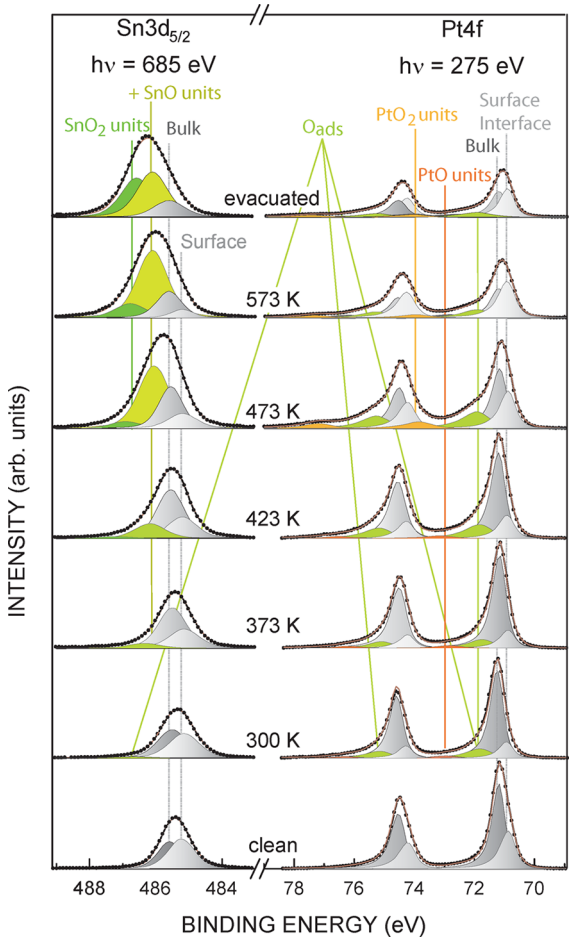

Figure 1. $Sn3d_{5/2}$ and Pt4f photoelectron spectra recorded on $Pt_3Sn(111)$-(2×2) during oxidation at different temperatures. O_{ads} represents the atomic oxygen chemisorbed in the H_{Pt2Sn}(Pt(fcc)) site described in the text. 500 mTorr O_2 was introduced at 300 K. The bottom spectrum was measured before oxygen was introduced and the top spectrum after evacuation of oxygen at room temperature.

the SI. When the coverage increases from 1/12 to 1/6 ML, the best adsorption form is a three-fold fcc hollow structure on a Pt_2Sn site (peak (1) in Figure 2) with an adsorption energy of −1.28 eV per oxygen atom weakly depending on the surface coverage. This adsorption site exhibits the lowest calculated CLBE for O1s and corresponds to the experimental binding energy (BE) of 529.25 eV. This electronic state will thus serve as a reference for the energy shifts. As exposed hereabove, two other components have been observed (530.15 and 531.4 eV). In the range of 1/12–1/6 ML coverage, molecular oxygen adsorption is possible according to DFT with an adsorption energy of −0.59 and −0.79 eV.[23] In the optimized structure, both oxygen atoms are associated with an average O1s BE shifted by +1.9 eV with respect to atomic oxygen adsorption. (See δ_{13} and structure (3) in Figure 2.) The coverage weakly modifies this shift. The corresponding electronic state assigned to molecular adsorption is fully compatible with the experimental component at 531.4 eV measured at 300 K (peak (3) in Figure 2 shifted by +2.2 eV with respect to peak (1)). At this temperature, the calculated rate constant for oxygen dissociation is significant (10^2 to 10^3 s^{-1}).[21] Hence the effective coverage of atomic oxygen might be larger than 1/6 ML. The picture related to atomic adsorption is even more complex for coverages larger than 1/6 ML. At 1/4 ML, three

dx.doi.org/10.1021/jz301802g | J. Phys. Chem. Lett. 2012, 3, 3707–3714

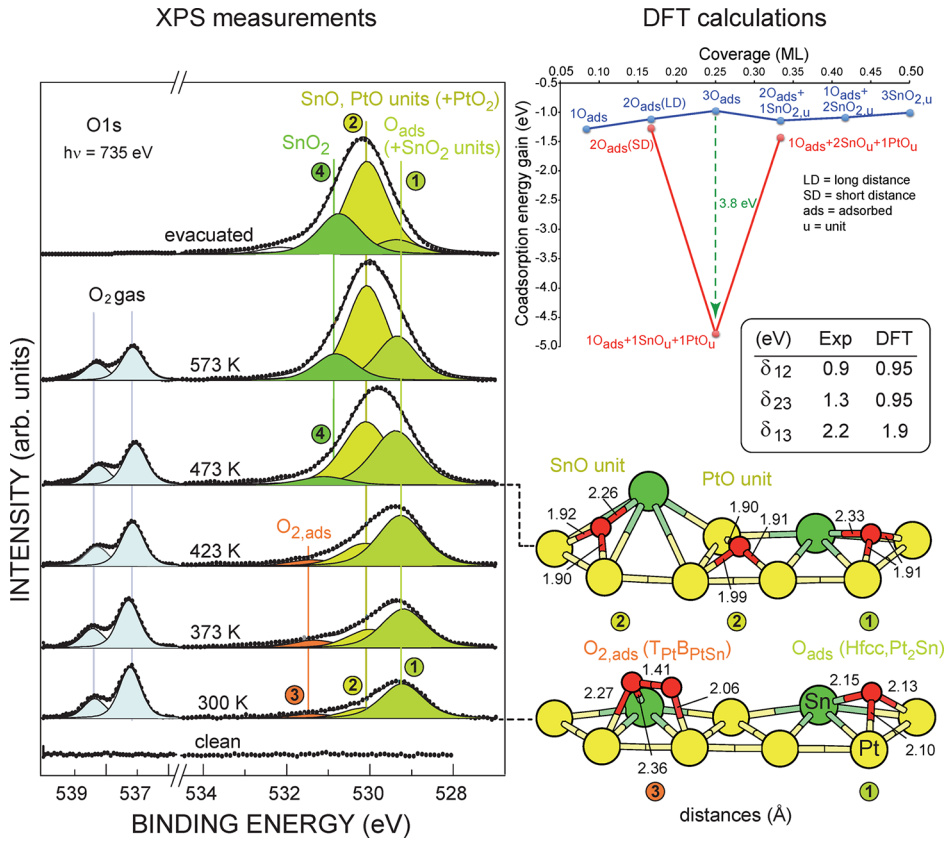

Figure 2. (left) O1s photoelectron spectra recorded during the oxidation of $Pt_3Sn(111)$-(2 × 2) at different temperatures and under 500 mTorr oxygen. (right) DFT calculations of the CLBE shifts of atomic and molecular adsorptions of oxygen on $Pt_3Sn(111)$-(2 × 2) and of the coadsorption energy gain (eV) between two oxygen adsorption states as a function of coverage. SnO and PtO units grown in an early stage are depicted.

oxygen atoms are chemisorbed in the supercell: one nonclassical adsorption structure with a strongly vertically relaxed surface Sn atom, one highly deformed Pt_3 hollow site, and one regular Pt_2Sn hollow position. This coadsorption at short distance exhibits a much larger energy gain (3.8 eV) than the chemisorption of three equidistant atoms. These new surface species named SnO and PtO units (see structure (2) in Figure 2) correspond to an early stage of the surface oxide growth. Such a PtO-like surface oxide phase was observed during oxidation of Pt(111).[4] The calculated average CLBE shift of 0.95 eV completely agrees with the measured shift between the medium-green and the light-green components. (See δ_{12} in Figure 2.) Hence the O1s component at 530.15 eV is unequivocally assigned to these low dimension surface oxides. For a coverage of 1/3 ML, a second SnO unit is obtained, although the energy gain with respect to coverage 1/4 ML is less (−1.4 eV). At this coverage, the adsorption of atomic oxygen can also lead to the formation of one SnO_2 surface species coadsorbed with two regular hollow adsorption sites.[23] This structure is, however, much less stable than the one evoked with two SnO and one PtO units. Because SnO_2 and atomic oxygen adsorption exhibit almost the same BE, SnO_2 cannot be excluded in the XPS measurements. These surface species can now be clearly identified on the corresponding Pt4f and Sn3d core levels. (See Figure 1.) The formation of PtO units induces a Pt4f component (BE = 73.0 eV) shifted by 1.85 eV relative to the surface component. The SnO unit "fingerprint" appears on $Sn3d_{5/2}$ at ∼486.1 eV (SCLS: 0.9 eV), overlapping the O_{ads} component. Between 300 and 423 K, these structures are stable on the surface. At 423 K, one can note an increased intensity of the Sn3d structure at 486.1 eV, which does not have its counterpart on the Pt4f level. Hence we can assign this component to SnO units. In this range of temperature, the three O1s components are stable and exhibit an increase in intensity except for the quasi-equivalent component assigned to molecular oxygen.

Heating beyond 473 K represents a new step in the oxidation process with the emergence of new structures at 73.85 eV (SCLS: 2.7 eV) for $Pt4f_{7/2}$ and at ∼486.7 eV (SCLS: 1.55 eV) for $Sn3d_{5/2}$. Pt4f core level shifts induced by further oxidation are expected to be about +1.1 eV for PtO and +2.9 eV for PtO_2 bulk oxides.[29,30] Clearly the new feature observed on Pt4f (SCLS 2.7 eV) is associated with the formation of PtO_2 units. The corresponding O1s structure is expected around 530.2 eV.[4,29] The Sn3d at 486.7 eV (SCLS = 1.55 eV) is associated with the formation of SnO_2-like species. From the literature, a shift of 1.5 to 1.8 eV is expected between Sn^{2+} and the zerovalent component.[31−34] In the meantime, the O1s spectrum shows simultaneously the extinction of molecular oxygen and the appearance of a new structure at 531.1 eV. Because this component behaves like the highest BE Sn3d (486.7 eV) when temperature is increased, it is assigned to SnO_2 in agreement with published data.[35] The possibility of a tin surface oxide layer SnO_x with oxygen atom defects has been ruled out on the basis of DFT. In fact, a (4 × 4) SnO_x structure proposed by Atrei and coworkers[36] has been fully optimized and the calculation of the O1s CLBE unequivocally indicates that, if present, defective tin surface oxide layers would provide lower BEs than the atomic oxygen component (∼1 eV below). However, this is not observed experimentally. The not

dx.doi.org/10.1021/jz301802g | J. Phys. Chem. Lett. 2012, 3, 3707−3714

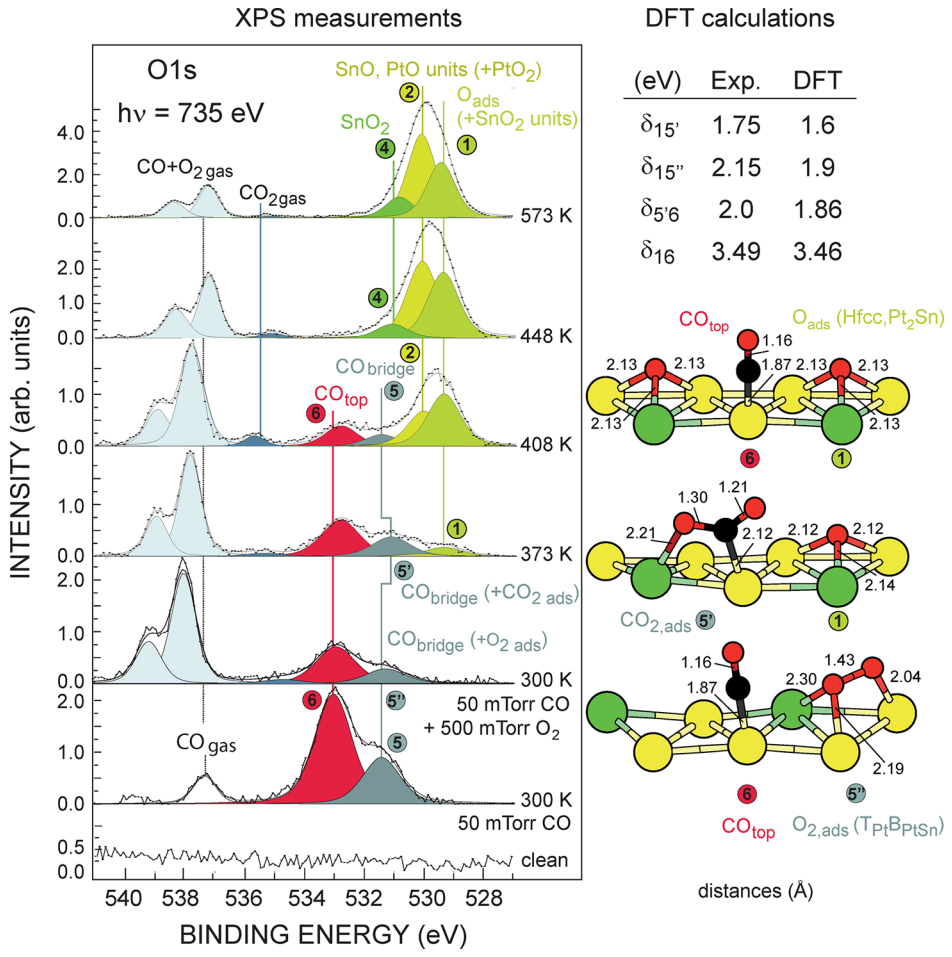

Figure 3. (left) Evolution of O1s photoelectron spectra with temperature on the (2 × 2) surface during CO oxidation with 50 mTorr CO, followed by 500 mTorr O_2. (right) DFT calculations of the CLBE shifts for CO and CO_2 adsorptions on $Pt_3Sn(111)$-(2 × 2) in the presence of molecular and atomic oxygen adsorptions.

complete disappearance of Pt4f and Sn3d surface components indicates that oxygen-free domains still exist on the surface at such a high pressure of O_2. A similar conclusion was reported by Batzill et al.[37] for the oxidized (2 × 2) Pt_3Sn surface alloy. These observations open the discussion of the coexistence of domains of pure Pt overlayers and SnO patches. Finally, after evacuation of the reactor and back to 300 K, the SnO_2 and PtO_2 units formed beyond 473 K under 500 mTorr O_2 remain on the surface.

In a second step, carbon monoxide oxidation is examined on the (2 × 2) surface. As shown in Figure 3, under 50 mTorr CO, beside the CO gas phase contribution observed at 537.4 eV, the O1s signal shows two components at 533.0 and 531.4 eV (peaks (6) and (5)) attributed to CO top and bridge adsorption, respectively. (See the SI for more details.) When 500 mTorr oxygen is added to CO, the O_2 gas doublet is shifted by 1 eV toward higher BE with respect to the previous case without CO partial pressure. (See Figure 2.) This shift is essentially due to adsorbed carbon monoxide on the metallic surface, which usually modifies the work function significantly (about 0.8 to 1.2 eV). A similar shift is expected for the CO_{gas} peak, which is now overlapped by the O1s gas phase doublet. At the same time, the top and bridge CO peak intensities decrease simultaneously due to the absorption by the surrounding gas phase. According to our interpretation of Figure 2, molecular oxygen adsorption should induce a structure at 531.4 eV, that is, in the CO bridge region. (See peak (5″).) At 300 K, no atomic oxygen adsorption is detected here, in contrast with previous results obtained under oxygen pressure alone. This means that the two possible sources of atomic oxygen (oxygen dissociation and carbon monoxide oxidation) are both turned off under these conditions. A temperature of 373 K is required to observe adsorbed atomic oxygen (O_{ads}) on this surface at 529.5 eV (peak (1) in Figure 3).

As in the case of oxygen dissociation, an interpretation of the XPS measurements for CO oxidation, is developed hereafter on the basis of DFT calculations.The DFT O1s BE shift δ_{16} between atomic oxygen (on Pt_2Sn hollow site) and CO top (on Pt) is +3.46 eV (see Figure 3) in very good agreement with the experimental shift (+3.46 eV). The theoretical shift $\delta_{15''}$ of +1.9 eV associated with molecular oxygen adsorption is reported in the Figure (peak (5″)) and compared with actual measurements (+2.15 eV), starting from 300 K. However, at this temperature we are not able to distinguish between bridge CO and molecular oxygen O1s peaks because they overlap. Between 300 and 373 K, the corresponding peak (5′) is shifted by −0.4 eV with respect to (5″), whereas the top CO remains unchanged according to XPS measurements. The presence of CO and atomic oxygen adsorbed on the surface raises the question of the beginning of CO oxidation and consequently of the formation of CO_2. Because no gas-phase CO_2 is detected

dx.doi.org/10.1021/jz301802g | J. Phys. Chem. Lett. 2012, 3, 3707−3714

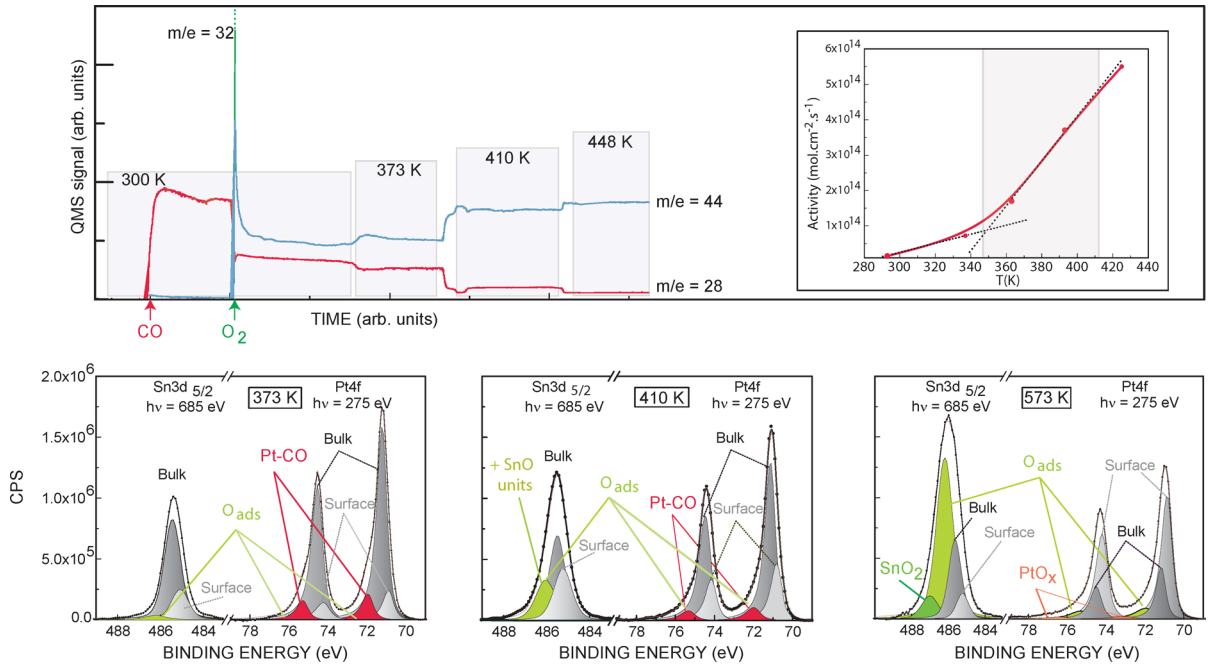

Figure 4. CO oxidation on the (2 × 2) surface at various temperatures: (top left) evolution of CO (m/e = 28), O_2 (m/e = 32), and CO_2 (m/e = 44) signals; (top right) evolution of the activity (mol cm^{-2} s^{-1}); (bottom) $Sn3d_{5/2}$ and Pt4f core levels measured at 373, 410, and 573 K with the initial conditions of 50 mTorr CO plus 500 mTorr O_2 introduced at 300 K. O_{ads} represents the atomic oxygen chemisorbed in the H_{Pt2Sn}(Pt(fcc)) site.

up to this temperature (373 K), only the adsorbed form of CO_2 could be at the origin of such a negative shift. This assumption is supported by DFT. The computed shift $\delta_{1S'}$ for CO_2 adsorption structure is +1.6 eV, a value fully compatible with the experimental shift of +1.75 eV observed for the structure (5′), which can thus be assigned to CO bridge and CO_2 adsorptions. Adsorbed carbon dioxide could have been detected here under significant partial pressures of reactants. Hence CO oxidation has started at 373 K; however, in this first regime, the turnover frequency is surely limited by the large CO coverage, leaving almost no free space for the reaction.

This picture is unequivocally changed when a small increase in temperature is operated. At 408 K, CO top (6) and bridge (5) O1s intensities tend to decrease with a large simultaneous increase in surface oxide species (see (1) and (2) in Figures 2 and 3). In addition, the CO bridge component (5) is shifted by +0.4 eV back to its initial position at 300 K. Finally, CO_2 is clearly detected in the gas phase (BE = 535.7 eV) at this temperature. All of these observations allow us to correlate the significant appearance of SnO and PtO units (structure (2)) to an increase in the catalytic activity toward CO oxidation, which is in turn linked to a decrease in adsorbed CO and CO_2 stability. In this context, the sudden growth of early stage surface oxides seems to increase significantly the surface oxygen coverage and promote CO oxidation by destabilizing CO adsorption state and consequently by lowering the activation barrier. This argument has been previously illustrated by DFT calculations of CO oxidation barriers as a function of spectator oxygen coverage.[21] The discussion related to the existence of a second catalytic regime will be examined by kinetic measurements later on.

A further increase in the sample temperature from 408 to 448 K brings once again a very interesting change of the catalytic behavior. At this temperature, CO adsorption states disappear completely while SnO_2-like surface oxides start to grow (peak (4) in Figure 4). At the same time, the gas-phase CO_2 component also decreases, which is clearly an indication of a fall of the catalytic activity. As a minor remark, CO desorption induces a reverse shift of the gas phase O1s components related to work function changes. At an even higher temperature (573 K), the PtSn surface seems to be totally deactivated toward CO oxidation. In this stage of the investigation of this catalytic system, several assumptions could be made to explain this passivation. In this third and last regime, either the desorption temperature of CO has been reached, hence hindering the reaction, or the presence of SnO_2 is responsible for CO desorption (high oxygen surface content and coverage).

A key point concerns the relation between the catalytic activity and the state of the surface during CO oxidation on $Pt_3Sn(111)$. Combining NAP-XPS and mass spectroscopy, one can now describe the surface chemistry on the working model $Pt_3Sn(111)$ catalyst through a correlation between the observed surface species and the reactivity. We report in Figure 4 the simultaneous evolution of the main core levels (Sn3d and Pt4f, in the bottom part) and of the gas-phase mass spectra (upper part) at different temperatures and, in particular, close to that of maximum activity reached on the (2 × 2) surface. The top right part of the Figure shows the evolution of activity during CO oxidation. Mass spectra show that even at 300 K the catalyst produces already some CO_2. This activity is slightly increased when temperature reaches 373 K. In this stage, top CO and atomic oxygen O_{ads} are coadsorbed on the surface (see the bottom part at 373 K). Increasing the temperature to 410−450 K enhances greatly the activity. In this range of temperature, the CO coverage has decreased, allowing the formation of SnO units (see bottom part at 410 K). At higher temperature, ca. 573 K, the decrease in activity is accompanied by a larger amount of SnO units and the emergence of SnO_2 and probably $PtO_{x<2}$ species, whereas no chemisorbed CO is observed anymore, probably due to a too short lifetime or residence time on the surface.

dx.doi.org/10.1021/jz301802g | J. Phys. Chem. Lett. 2012, 3, 3707−3714

Because CO interacts only with Pt atoms,[20] CO oxidation would then occur on a Pt site at the perimeter of the oxidic SnO_x domains grown on top of the catalyst. The reducing properties of CO probably restrict the extension of the SnO_x domains during CO oxidation. These results are fully compatible with very recent literature data concerning CO oxidation (under UHV conditions) on nanostructured SnO_x on Pt(111) surfaces.[38] Deactivation occurs when the coverage or the residence time of CO on the surface is too small (temperature driven), allowing a more extended or deeper oxidation of the surface with a partial surface dealloying.

In the following final discussion, a comparative quantitative analysis of (2 × 2) and ($\sqrt{3} \times \sqrt{3}$) surfaces is presented in Figure 5. Regarding tin segregation (Sn/Pt atomic ratio), it

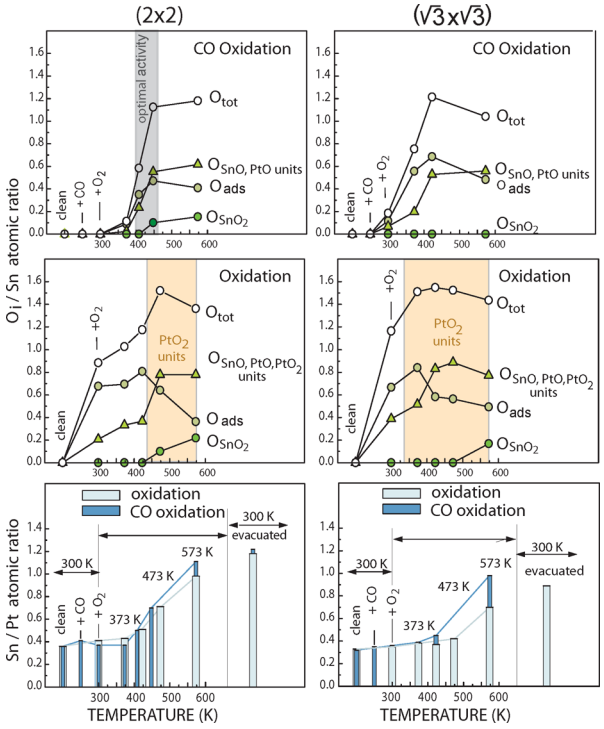

Figure 5. O_i/Sn (top and middle), and Sn/Pt (bottom) atomic ratio evolution during oxidations at different temperatures on $Pt_3Sn(111)$-(2 × 2) (left) and $Pt_3Sn(111)$-($\sqrt{3} \times \sqrt{3}$) (right) surfaces. O_i corresponds to O atoms involved in the chemisorbed phase O_{ads}, to oxidic species (SnO, PtO, and PtO_2 units), or to domains of SnO_2 species. O_{tot} is the summation over all O1s components. The presence of PtO_2 is mentioned by the yellow-shaded areas, and the optimal activity for CO oxidation is mentioned by the gray-shaded zone.

increases with temperature on both surfaces (see bottom part). However, a deeper restructuring occurs on the (2 × 2) because the segregation starts at a lower temperature and to a larger extent. This difference might be explained by an intrinsic lower Sn content in the first sublayers of the ($\sqrt{3} \times \sqrt{3}$) (41 Sn at % versus 49). Furthermore, tin segregation is promoted by the presence of gaseous CO above 400 K (zero CO coverage).

The middle part of the Figure refers to the direct oxidation of $Pt_3Sn(111)$ surfaces on top of which the same SnO, SnO_2, PtO, and PtO_2 units were observed. The domain of temperature for which PtO_2 units were detected is schematized by yellow-shaded rectangles. These units appear at a lower temperature on the ($\sqrt{3} \times \sqrt{3}$) surface (350 K versus 423 K). Similarly more SnO, SnO_2, PtO, and PtO_2 units are formed between 300 and 425 K on this termination. As temperature is increased, Sn and Pt are oxidized either simultaneously on the (2 × 2) surface (SnO_2 and PtO_2 units) at ∼473 K or sequentially (PtO_2 first at ∼350 K, and then SnO_2 for temperatures higher than 473 K) on the ($\sqrt{3} \times \sqrt{3}$) surface. Whether the SnO_2 and PtO_2 units wet the alloy surface or form particles remains up to now unanswered.

The gray-shaded area reported in the top-left part reminds us that the best activity in CO oxidation was obtained on the (2 × 2) at 425 K.[21] It also corresponds to the temperature range of highest production of CO_2 in the present work. The total oxygen uptake (O_{tot}/Sn atomic ratio) is greatly reduced by the presence of CO until ∼400 K, that is, before CO desorption. The SnO and SnO_2 units are formed at higher temperature in the presence of CO. In contrast with direct oxidation, no surface PtO_2 is observed here, which means that if formed it is readily reduced by CO. Indeed, under elevated pressure (CO +O_2), Pt_3Sn is converted into a so-called "inverse catalyst" by analogy to supported catalysts,[39] that is, an oxide (SnO_x)-on-metal (Pt_3Sn) interface. One can also notice the formation of SnO_2 units on the (2 × 2) surface only, beyond 400 K. Finally, looking at the (SnO+PtO units) O1s component, it increases more rapidly on the ($\sqrt{3} \times \sqrt{3}$) surface when temperature is increased. This is confirmed by Sn3d peak decomposition, which indicates that at 373 K, 26 and 34% of tin atoms are oxidized into SnO_x on the (2 × 2) and on the ($\sqrt{3} \times \sqrt{3}$), respectively. In the range 425−450 K, SnO_x represents already 57% of the total tin on the ($\sqrt{3} \times \sqrt{3}$), whereas it is only 45% on the (2 × 2). This is in agreement with the competitive adsorption of carbon monoxide and oxygen on this surface[20] and could explain why the (2 × 2) is more active at this temperature than the ($\sqrt{3} \times \sqrt{3}$). Too many SnO units on the surface reduce the number of available sites for CO chemisorption and further oxidation.

In conclusion, synchrotron-radiation-based NAP-XPS has been used to investigate the evolution of the $Pt_3Sn(111)$-(2 × 2) and -($\sqrt{3} \times \sqrt{3}$) surfaces during CO oxidation with a high surface sensitivity. Various conditions of oxygen and CO pressure have been considered in the range of a few hundred millitorr. In addition, DFT calculations of O1s CLBE have been performed to shed light on the interpretation. This work demonstrates the formation of early stage grown surface oxides in a complex catalytic system. In contrast with previous UHV studies, molecular oxygen is dissociated on this bimetallic surface under elevated pressure. Under direct oxidation condition, the surface composition is modified significantly. Tin segregates to the surface on both surfaces and to a larger extent on the (2 × 2). Sn and Pt are progressively oxidized into SnO, PtO, SnO_2, and PtO_2 surface units. Three different catalytic regimes have been identified during CO oxidation on the (2 × 2) surface and interpreted with the help of DFT simulations. At 300 K, the catalytic activity is low and the active phase is an effective bimetallic PtSn system. The reaction mechanism is the classical picture with coadsorbed CO and atomic oxygen. Under these conditions, for the first time, molecular adsorption of CO_2 could be detected with CO bridge competitive adsorption forms. A moderate increase in the temperature (350−450 K) changes the catalytic behavior. In the second regime, the catalytic activity is significantly enhanced. Because of the temperature and the formation of early stage grown surface oxides (SnO and PtO units), there is a simultaneous destabilization of CO adsorption and desorption of CO_2. According to the DFT models, this is

dx.doi.org/10.1021/jz301802g | J. Phys. Chem. Lett. 2012, 3, 3707−3714

fully compatible with a decrease in the activation energy barrier for CO oxidation. At an even higher temperature (~550 K), the catalytic activity starts to decrease. Under optimal catalytic conditions, the structure of the Pt_3Sn surface is partially covered by SnO units. This reverse picture with respect to the usual oxide supported metallic particles recalls an "inverse catalyst". This opens interesting perspectives regarding the catalytic activity of such metal-supported SnO species.

■ ASSOCIATED CONTENT

Supporting Information

More details of experiment and theory methods, XPS of the clean surfaces, NAP-XPS of $Pt_3Sn(111)$-$(\sqrt{3} \times \sqrt{3})$ oxidation and CO oxidation of both surfaces under CO pressure, DFT CLBE for oxygen dissociation, atomic oxygen adsorption, and CO oxidation. This material is available free of charge via the Internet at http://pubs.acs.org.

■ AUTHOR INFORMATION

Corresponding Author

*E-mail: yjugnet@gmail.com.

Notes

The authors declare no competing financial interest.

■ ACKNOWLEDGMENTS

This research was partially carried out at the Advanced Light Source supported by the Director, Office of Science, Office of Basic Energy Sciences, U.S. Department of Energy under contract DE-AC02-05CH11231. Y.J. acknowledges U. Bardi (Firenze University) for providing the $Pt_3Sn(111)$ sample and the Agence Nationale de la Recherche (ANR) for financial support (ANR-08-BLAN-0096-03). D.L., C.D., and F.D. thank IDRIS, Orsay, CINES, Montpellier and PSMN, Lyon for CPU time and assistance.

■ REFERENCES

(1) Over, H.; Seitsonen, A. Oxidation of Metal Surfaces. *Science* **2002**, *297*, 2003−2005.

(2) Gustafson, J.; Westerström, R.; Resta, A.; Mikkelsen, A.; Andersen, J. N.; Balmes, O.; Torrelles, X.; Schmid, M.; Varga, P.; Hammer, B.; Kresse, G.; Baddeley, C.; Lundgren, E. Structure and Catalytic Reactivity of Rh Oxides. *Catal. Today* **2009**, *145*, 227−235.

(3) Knudsen, J.; Merte, L. R.; Peng, G.; Vang, R. T.; Resta, A.; Lægsgaard, E.; Andersen, J. N.; Mavrikakis, M.; Besenbacher, F. Low-Temperature CO Oxidation on Ni(111) and on a Au/Ni(111) Surface Alloy. *ACS Nano* **2010**, *4*, 4380−4387.

(4) Miller, D. J.; Öberg, H.; Kaya, S.; Sanchez-Casalongue, H.; Friebel, D.; Anniyev, T.; Ogasawara, H.; Bluhm, H.; Pettersson, L. G. M.; Nilsson, A. Oxidation of Pt(111) under Near-Ambient Conditions. *Phys. Rev. Lett.* **2011**, *107*, 195502.

(5) Gustafson, J.; Westerström, R.; Balmes, O.; Resta, A.; van Rijn, R.; Torrelles, X.; Herbschleb, C. T.; Frenken, J. W. M.; Lundgren, E. Catalytic Activity of the Rh Surface Oxide: CO Oxidation over Rh(111) under Realistic Conditions. *J. Phys. Chem. C* **2010**, *114*, 4580−4583.

(6) Gao, F.; Goodman, D. W. CO Oxidation over Ruthenium: Identification of the Catalytically Active Phases at near-Atmospheric Pressures. *Phys. Chem. Chem. Phys.* **2012**, *14*, 6688−6697.

(7) Butcher, D. R.; Grass, M. E.; Zeng, Z.; Aksoy, F.; Bluhm, H.; Li, W. X.; Mun, B. S.; Somorjai, G. A.; Liu, Z. In Situ Oxidation Study of Pt(110) and Its Interaction with CO. *J. Am. Chem. Soc.* **2011**, *133*, 20319−20325.

(8) Sun, Y. N.; Qin, Z. H.; Lewandowski, M.; Kaya, S.; Shaikhutdinov, S.; Freund, H. J. When an Encapsulating Oxide Layer Promotes Reaction on Noble Metals: Dewetting and In situ Formation of an Inverted FeO_x/Pt Catalyst. *Catal. Lett.* **2008**, *126*, 31−35.

(9) Toyoshima, R.; Yoshida, M.; Monya, Y.; Kousa, Y.; Susuki, K.; Abe, H.; Mun, B. S.; Mase, K.; Ameniya, K.; Kondoh, H. In Situ Ambient Pressure XPS Study of CO Oxidation Reaction on Pd(111) Surfaces. *J. Phys. Chem. C* **2012**, *116*, 18691−18697.

(10) Speller, S.; Bardi, U. Chapter IV, Surface Alloys and Alloy Surfaces: The Platinum-Tin System. In *The Chemical Physics of Solid Surfaces*; Woofruff, D. P., Ed.; Elsevier: New York, 2002; Vol. *10*.

(11) Atrei, A.; Bardi, U.; Wu, J.; Zanazzi, E.; Rovida, G. LEED Crystallographic Investigation of Ultrathin Films Formed by Deposition of Sn on the Pt(111) Surface. *Surf. Sci.* **1993**, *290*, 286−294.

(12) Dupont, C.; Jugnet, Y.; Loffreda, D. Theoretical Evidence of PtSn Alloy Efficiency for CO Oxidation. *J. Am. Chem. Soc.* **2006**, *128*, 9129−9136.

(13) Dupont, C.; Loffreda, D.; Delbecq, F.; Jugnet, Y. Vibrational Study of CO Chemisorption on the $Pt_3Sn(111)$-(2×2) Surface. *J. Phys. Chem. C* **2007**, *111*, 8524−8531.

(14) Dupont, C. A Model Surface Approach to CO Oxidation Aiming at the Purification of H_2 Combustible: The $Pt_3Sn(111)$ Surface Investigated by HREELS, PM-IRRAS and DFT. Ph.D. Thesis, Lyon University, 2008.

(15) Paffett, M. T.; Gebhard, S. C.; Windham, R. G.; Koel, B. E. Chemisorption of Carbon Monoxide, Hydrogen, And Oxygen on Ordered Tin/Platinum(111) Surface Alloys. *J. Phys. Chem.* **1990**, *94*, 6831−6839.

(16) Unger, W.; Marton, D. A; Sims, X. P. S. Examination of Low-Pressure Oxygen Adsorption on Pt_3Sn: Oxygen Uptake and Surface Characteristics. *Surf. Sci.* **1989**, *218*, L467−L475.

(17) Hoheisel, M.; Speller, S.; Atrei, A.; Bardi, U.; Rovida, G. Adsorption of Oxygen on $Pt_3Sn(110)$ Studied by STM and LEED. *Phys. Rev. B* **2005**, *71*, 35410.

(18) Saliba, N. A.; Tsai, Y. L.; Koel, B. E. Oxidation of Ordered Sn/Pt(111) Surface Alloys and Thermal Stability of the Oxides Formed. *J. Phys. Chem. B* **1999**, *103*, 1532−1541.

(19) Batzill, M.; Kim, J.; Beck, D. E.; Koel, B. E. Epitaxial Growth of Tin Oxide on Pt(111): Structure and Properties of Wetting Layers and SnO_2 Crystallites. *Phys. Rev. B* **2004**, *69*, 165403.

(20) Dupont, C.; Loffreda, D.; Delbecq, F.; Aires, F. C. S.; Erhet, E.; Jugnet, Y. A High Pressure PM-IRRAS Study of CO and O_2 Coadsorption and Reactivity on PtSn Alloy Surfaces. *J. Phys. Chem. C* **2008**, *112*, 10862−10867.

(21) Dupont, C.; Jugnet, Y.; Delbecq, F.; Loffreda, D. Mediatory Role of Tin in the Catalytic Performance of Tailored Platinum-Tin Alloy Surfaces for Carbon Monoxide Oxidation. *J. Catal.* **2010**, *273*, 211−220.

(22) Jerdev, D. I.; Koel, B. E. Oxidation of Ordered Pt-Sn Surface Alloys by O_2. *Surf. Sci.* **2001**, *492*, 106−114.

(23) Dupont, C.; Jugnet, Y.; Delbecq, F.; Loffreda, D. Restructuring of the $Pt_3Sn(111)$ Surfaces Induced by Atomic and Molecular Oxygen from First Principles. *J. Chem. Phys.* **2009**, *130*, 124716.

(24) Grass, M. E.; Karlsson, P. G.; Aksoy, F.; Lundqvist, M.; Wannberg, B.; Mun, B. S.; Hussain, Z.; Liu, Z. New Ambient Pressure Photoemission Endstation at Advanced Light Source Beamline 9.3.2. *Rev. Sci. Instrum.* **2010**, *81*, 053106.

(25) Kresse, G.; Hafner, J. Ab Initio Molecular Dynamics for Liquid Metals. *Phys. Rev. B* **1993**, *47*, 558−561.

(26) Kresse, G.; Furthmüller, J. Efficient Iterative Schemes for Ab Initio Total-Energy Calculations Using a Plane-Wave Basis Set. *Phys. Rev. B* **1996**, *54*, 11169−11186.

(27) Perdew, J. P.; Burke, K.; Ernzerhof, M. Generalized Gradient Approximation Made Simple. *Phys. Rev. Lett.* **1996**, *77*, 3865−3868.

(28) Kresse, G.; Joubert, D. From Ultrasoft Pseudopotentials to the Projector Augmented-Wave Method. *Phys. Rev. B* **1999**, *59*, 1758−1775.

(29) Peuckert, M.; Bonzel, H. P. Characterization of Oxidized Platinum Surfaces by X-ray Photoelectron Spectroscopy. *Surf. Sci.* **1984**, *145*, 239−289.

(30) Parkinson, C.; Walker, M.; McConville, C. Reaction of Atomic Oxygen with a Pt(1 1 1) Surface: Chemical and Structural Determination Using XPS, CAICISS and LEED. *Surf. Sci.* **2003**, *545*, 19−33.
(31) Themlin, J. M.; Chtaib, M.; Henrard, L.; Lambin, P.; Darville, J.; Gilles, J. Characterization of Tin Oxides by X-ray-Photoemission Spectroscopy. *Phys. Rev. B* **1992**, *46*, 2460−2466.
(32) Jie, L.; Chao, X. XPS Examination of Tin Oxide on Float Glass Surface. *J. Non-Cryst. Solids* **1990**, *119*, 37−40.
(33) Padova, P. D.; Fanfon, M.; Larciprete, R.; Mangiantini, M.; Priori, S.; Perfetti, P. A Synchrotron Radiation Photoemission Study of the Oxidation of Tin. *Surf. Sci.* **1994**, *313*, 379−391.
(34) Szuber, J.; Czempik, G.; Larciprete, R.; Koziej, D.; Adamowicz, B. XPS Study of the L-CVD Deposited SnO_2 Thin Films Exposed to Oxygen and Hydrogen. *Thin Solid Films* **2001**, *391*, 198−203.
(35) Liu, W.; Cao, X.; Zhu, Y.; Cao, L. The Effect of Dopants on the Electronic Structure of SnO_2 Thin Film. *Sens. Actuators, B* **2000**, *66*, 219−221.
(36) Atrei, A.; Bardi, U.; Rovida, G.; Torrini, M.; Hoheisel, M.; Speller, S. Test of Structural Models for the (4×4) Phase Formed by Oxygen Adsorption on the $Pt_3Sn(1\ 1\ 1)$ Surface. *Surf. Sci.* **2003**, *526*, 193−200.
(37) Batzill, M.; Beck, D. E.; Jerdev, D.; Koel, B. E. Tin-Oxide Overlayer Formation by Oxidation of Pt-Sn(111) Surface Alloys. *J. Vac. Sci. Technol., A* **2001**, *19*, 1953−1958.
(38) Axnanda, S.; Zhou, W. P.; White, M. G. CO Oxidation on Nanostructured SnO_x/Pt(111) Surfaces: Unique Properties of Reduced SnO_x. *Phys. Chem. Chem. Phys.* **2012**, *14*, 10207−10214.
(39) Leisenberger, F. P.; Surnev, S.; Koller, G.; Ramsey, M. G.; Netzer, F. P. Probing the Metal Sites of a Vanadium Oxide - Pd(111) Inverse Catalyst: Adsorption of CO. *Surf. Sci.* **2000**, *444*, 211−220.